

Differential activity-dependent regulation of the lateral mobilities of AMPA and NMDA receptors

Laurent Groc¹, Martin Heine¹, Laurent Cognet², Kieran Brickley³, F Anne Stephenson³, Brahim Lounis² & Daniel Choquet¹

The basis for differences in activity-dependent trafficking of AMPA receptors (AMPA) and NMDA receptors (NMDAR) remains unclear. Using single-molecule tracking, we found different lateral mobilities for AMPARs and NMDARs: changes in neuronal activity modified AMPAR but not NMDAR mobility, whereas protein kinase C activation modified both. Differences in mobility were mainly detected for extrasynaptic AMPARs, suggesting that receptor diffusion between synaptic and extrasynaptic domains is involved in plasticity processes.

Activity-dependent trafficking of AMPARs during synaptic plasticity processes relies on regulation of both receptor recycling through exocytosis-endocytosis¹ and lateral diffusion². NMDARs are also mobile

at the surface of neurons³, but they are considered to be less so than AMPARs⁴. Here, we directly compared the lateral mobilities of AMPARs and NMDARs. For this, we measured the diffusion of GluR2 subunit-containing AMPAR⁵ and NR1 subunit-containing NMDAR⁶ at the surface of cultured hippocampal neurons at 9–11 days *in vitro* (d.i.v.) by single-molecule fluorescence microscopy tracking of receptors labeled with appropriate Cy3-coupled antibodies⁵ (see **Supplementary Methods** online).

We constructed trajectories of single molecules from image series acquired at a rate of 15 Hz and calculated the instantaneous diffusion coefficient (D)⁵ (**Supplementary Methods**). To differentiate synaptic from extrasynaptic receptors, we labeled synapses with a rhodamine derivative of a mitochondrial marker⁵ (Red Deep Mitotracker); molecules located <300 nm from the center of a synapse were referred as 'synaptic'⁵ (**Supplementary Fig. 1**).

We compared AMPAR diffusion obtained with Cy3-conjugated antibodies (Fig. 1a,c) with semiconductor quantum dot (QD)-coupled antibodies, because QDs are more photostable than organic dyes⁷ (**Supplementary Fig. 2**). In the extrasynaptic membrane, diffusion distributions measured using Cy3-conjugated and QD-coupled antibodies were similar ($P = 0.34$) (**Supplementary Fig. 2**), thus validating the diffusion estimates obtained with Cy3-conjugated antibodies. Distributions of synaptic receptor diffusions were significantly different, however ($P < 0.0001$), with QD-coupled receptor diffusion being five times slower. This effect could be due to limitation of receptor diffusion within the glutamatergic synaptic cleft by the bound QD (QD diameter >10–15 nm) (but see ref. 7). Therefore, in the present study, AMPAR and NMDAR diffusions were estimated only from Cy3-conjugated antibodies.

Under basal conditions, diffusions of extrasynaptic AMPARs and NMDARs were significantly different ($P < 0.001$) (Fig. 1a,b). The

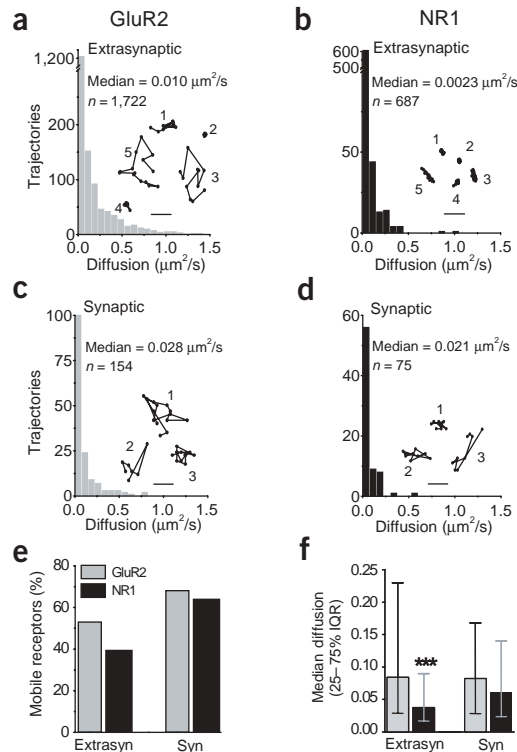


Figure 1 Differential lateral diffusion of AMPARs (■) and NMDARs (■) at the surface of 10-d.i.v. hippocampal neurons. Because AMPARs and NMDARs undergo exocytosis-endocytosis cycling^{1,12,13}, we carried out controls to show that the vast majority of labeled receptors were located at the surface of neurons during recording sessions (**Supplementary Methods**). (a,b) Histograms of extrasynaptic AMPAR (a) and NMDAR diffusions (b) (median value and number of reconstructed traces; bin size, 0.075 $\mu\text{m}^2/\text{s}$). AMPAR diffusion was approximately four times higher than NMDAR ($P < 0.0001$). Insets, examples of GluR2R (a) and NR1R (b) trajectories (bars, 100 nm). Average trajectory length (\pm s.d.) is 455 ± 520 ms, range 260–9,750 ms ($n = 643$). (c,d) Diffusion histograms of synaptic AMPARs and NMDARs. (e) Fractions of mobile AMPARs and NMDARs. Note the smaller fraction of mobile receptors in extrasynaptic membranes. Immobile receptors were defined as those with $D < 0.0075 \mu\text{m}^2/\text{s}$. (f) Median diffusion (± 25 –75% interquartile range) of mobile AMPAR (extrasynaptic, $n = 919$; synaptic, $n = 107$) and NMDAR (extrasynaptic, $n = 272$; synaptic, $n = 49$). (Mann-Whitney test, *** $P < 0.0001$).

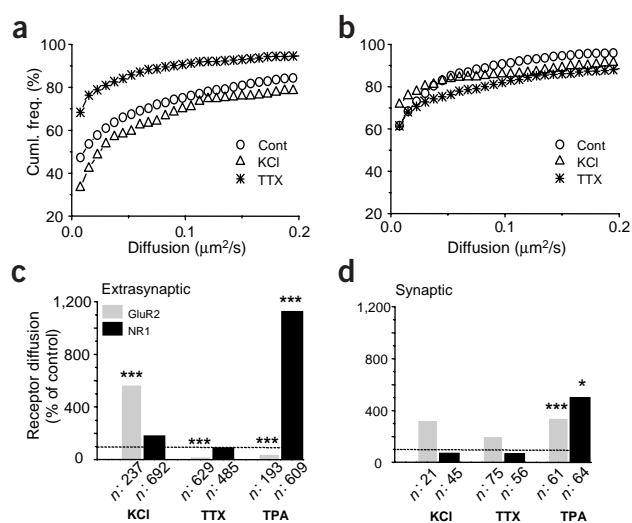
¹UMR 5091 CNRS–Université Bordeaux 2, Bordeaux 33077, France. ²CNRS-UMR 5798, Talence, France. ³School of Pharmacy, University of London, London, UK. Correspondence should be addressed to D.C. (dchoquet@u-bordeaux2.fr).

Figure 2 Neuronal activity differentially regulates AMPAR and NMDAR lateral diffusions. (a,b) Cumulative distributions of extrasynaptic AMPAR (a) and NMDAR (b) diffusions in control (○), 40 mM KCl (△) and 1 μM TTX (*) conditions. The first point of the distributions corresponds to the percentage of immobile receptors. (c,d) Bars, percentage change of AMPAR (■) and NMDAR median values (■) with respect to internal controls measured for each condition. (c) Effect of KCl, TTX and TPA on mobility of extrasynaptic receptors. Note the fivefold increase (to 560% of control) and eightfold decrease (to 12% of control) in extrasynaptic AMPAR diffusion after KCl and TTX treatment, respectively. Notably, NMDAR diffusion is statistically unchanged in the same conditions ($P > 0.05$). TPA increases NMDAR diffusion but decreases AMPAR diffusion. (d) Effect of the same treatments on synaptic receptor mobility. Neither KCl ($P > 0.12$) nor TTX treatment ($P > 0.84$) affected either AMPAR or NMDAR diffusion (Mann-Whitney test, *** $P < 0.0001$, * $P < 0.05$).

proportions of mobile AMPARs and NMDARs were similar (Fig. 1e), indicating that this difference was due mostly to slower diffusion of the mobile NMDARs as compared to the AMPARs (GluR2 median = $0.084 \mu\text{m}^2/\text{s}$, IQR = $0.028\text{--}0.23 \mu\text{m}^2/\text{s}$, $n = 919$; NR1 median = $0.037 \mu\text{m}^2/\text{s}$, IQR = $0.017\text{--}0.09 \mu\text{m}^2/\text{s}$, $n = 272$; $P < 0.001$) (Fig. 1f). When examined within synapses, diffusions of AMPARs and NMDARs were not significantly different (Fig. 1c,d) either in the proportion or the diffusion of the mobile receptors (Fig. 1e,f). Thus, under basal conditions, extrasynaptic AMPARs are more mobile than NMDARs, whereas mobility within synapses is undistinguishable.

Activation of hippocampal neurons through short-term application of glutamate increased AMPAR diffusion⁵, whereas local release of intracellular calcium produced the opposite effect⁸, indicating that neuronal activity can regulate lateral diffusion of AMPARs. We treated neurons with either potassium chloride (KCl, 40 mM) or tetrodotoxin (TTX, 1 μM) to increase or decrease neuronal activity, respectively. After 2 min of 40 mM KCl treatment, extrasynaptic AMPAR diffusion greatly increased (560% of control, $P < 0.001$), mainly owing to a decrease in the percentage of immobile receptors (from 47% to 32%, Fig. 2a,c). Notably, the AMPAR diffusion measured after KCl treatment (median $0.06 \mu\text{m}^2/\text{s}$, $n = 237$) is comparable to the previously published 'control' value (median $0.11 \mu\text{m}^2/\text{s}$, $n = 309$) obtained after similar KCl treatment needed to stain synapses with FM1-43 (ref. 5). When the spontaneous neuronal activity was blocked with TTX for only 10 min, no change in diffusion was observed^{15,8}; data not shown), consistent with the low spontaneous basal activity of our cultured neurons. However, blocking neuronal activity for 48 h greatly decreased extrasynaptic AMPAR diffusion (12% of control, $P < 0.001$), mainly owing to an increase in the percentage of immobile receptors (from 47% to 67%, Fig. 2a,c). Thus, extrasynaptic AMPAR diffusion was strongly affected by changes in neuronal activity. Less variation in AMPAR diffusion was detected inside than outside synapses (Fig. 2d). However, AMPARs freed from stabilization at synapses have a high chance of escaping the synapse and thus becoming part of the extrasynaptic pool of receptors⁹. Thus, increases in receptor mobility, whether inside or outside the synapse, are better detected within the extrasynaptic membrane. Neither 40 mM KCl nor 48 h TTX treatment affected synaptic or extrasynaptic NMDAR diffusion (Fig. 2).

Activation of protein kinase C (PKC) induces rapid dispersal of NMDARs from a clustered to a uniform membrane distribution¹⁰ as well as endocytosis and redistribution of GluR2-containing AMPARs to synaptic sites¹¹. We thus investigated whether NMDAR and AMPAR mobilities were affected by the PKC agonist 12-O-tetradecanoylphorbol (TPA). Neurons were treated for 5–20 min with either TPA (100 nM) or the inactive derivative 4- α -PHR (isophorbol, 100 nM). After TPA treatment, NMDAR diffusion was increased in both



extrasynaptic (12-fold, 1,200% of control, $P < 0.001$) and synaptic membranes (5-fold, 500% of control, $P < 0.05$) (Fig. 2a,b). This is consistent with the reported TPA-induced dispersion of NMDARs¹⁰. Extrasynaptic and synaptic AMPAR diffusions were also significantly affected by TPA treatment, but the effects were smaller than for NMDARs: $D = 34\%$ and $D = 333\%$ of control, respectively (Fig. 2a,b).

In summary, AMPARs and NMDARs diffuse differentially within the extrasynaptic membrane and neuronal activity specifically affects AMPAR diffusion. Our data further strengthen the hypothesis that the pool of extrasynaptic receptors may act as a reserve that can be mobilized on demand², making the extrasynaptic domain a trafficking hallway. The relative instability of the AMPAR with respect to the NMDAR synaptic component during plasticity⁴ may originate from greater lateral exchange of AMPARs at equilibrium between the synaptic and extrasynaptic domains.

Note: Supplementary information is available on the Nature Neuroscience website.

ACKNOWLEDGMENTS

We thank D. Bouchet for hippocampal neuron cultures. This work was supported by grants from Conseil Régional d'Aquitaine, the European Community (QLG3-CT-2001-02089) and the BBSRC (UK).

COMPETING INTERESTS STATEMENT

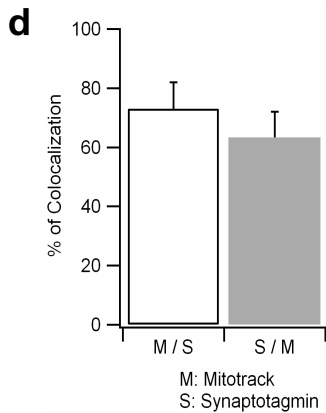
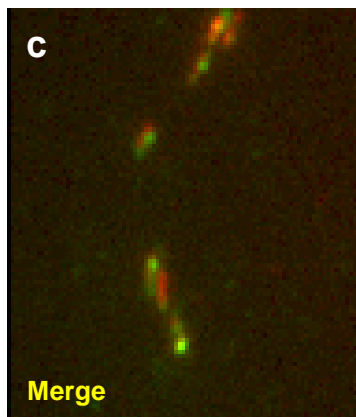
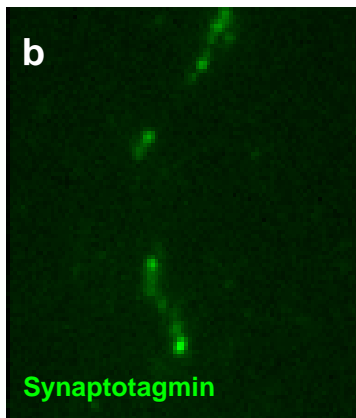
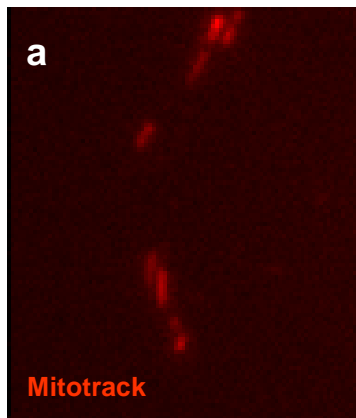
The authors declare that they have no competing financial interests.

Received 19 March; accepted 27 April 2004

Published online at <http://www.nature.com/natureneuroscience/>

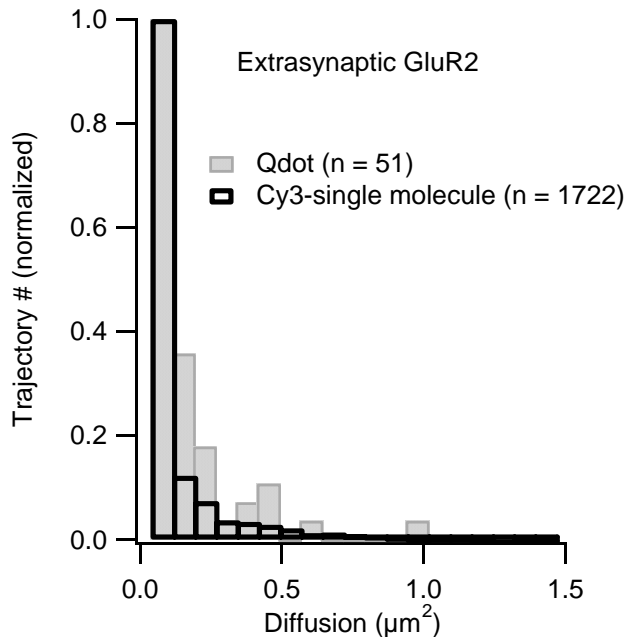
- Carroll, R.C., Beattie, E.C., von Zastrow, M. & Malenka, R.C. *Nat. Rev. Neurosci.* **2**, 315–324 (2001).
- Choquet, D. & Triller, A. *Nat. Rev. Neurosci.* **4**, 251–265 (2003).
- Tovar, K.R. & Westbrook, G.L. *Neuron* **34**, 255–264 (2002).
- Bredt, D.S. & Nicoll, R.A. *Neuron* **40**, 361–379 (2003).
- Tardin, C., Cognet, L., Bats, C., Lounis, B. & Choquet, D. *EMBO J.* **22**, 4656–4665 (2003).
- Racca, C., Stephenson, F.A., Streit, P., Roberts, J.D. & Somogyi, P. *J. Neurosci.* **20**, 2512–2522 (2000).
- Dahan, M. *et al. Science* **302**, 442–445 (2003).
- Borgdorff, A.J. & Choquet, D. *Nature* **417**, 649–653 (2002).
- Zhou, Q., Xiao, M. & Nicoll, R.A. *Proc. Natl. Acad. Sci. USA* **98**, 1261–1266 (2001).
- Fong, D.K., Rao, A., Crump, F.T. & Craig, A.M. *J. Neurosci.* **22**, 2153–2164 (2002).
- Chung, H.J., Xia, J., Scannevin, R.H., Zhang, X. & Huganir, R.L. *J. Neurosci.* **20**, 7258–7267 (2000).
- Wentholt, R.J., Prybylowski, K., Standley, S., Sans, N. & Petralia, R.S. *Annu. Rev. Pharmacol. Toxicol.* **43**, 335–358 (2003).
- Ehlers, M.D. *Neuron* **28**, 511–525 (2000).

Supplementary Figure 1

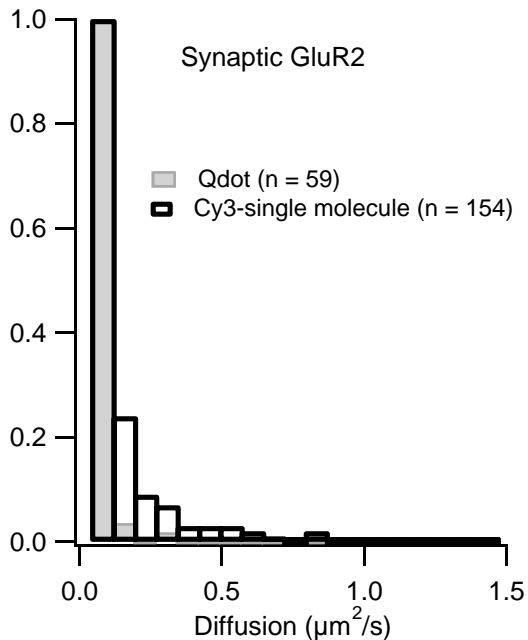


Supplementary Figure 2

a



b



Supplementary Methods (see also¹)

Cell culture, GluR2, NR1 and synapse staining

Hippocampal neurons from 18 day old rat embryos were cultured until 9-11 DIV on glass coverslips following the Banker technique as previously described² (density of ~5000 neurons/cm²). First, images of neurites were taken by differential interference contrast (DIC) to ascertain specific synaptic and receptor localization. Then, to label synapses, neurons were incubated for 1-2 min at 20°C with 1 nM Mitotracker (Deep Red-Fluorescent Mitotracker, Molecular Probes, Leiden, The Netherlands), a dye that does not require cell depolarization as compared to the commonly used FM1-43 dye. Cy3 was coupled to the antibodies at a mean ratio of 1:1 using the Cy3 mono-reactive dye pack (Amersham Biosciences, UK). We used the mouse monoclonal anti-GluR2 (BD Pharmingen, California, USA) and affinity-purified rabbit polyclonal anti-NR1 pan antibodies^{1,2,3} that are both directed against extracellular epitopes of the GluR2 and NMDAR-1 subunits respectively. Then, neurons were incubated for 10 min at 37°C with anti-GluR2-Cy3 or anti-NR1-Cy3. After a few rinses, coverslips were mounted in a custom chamber with culture medium at 37°C. For the high KCl conditions, neurons were incubated with 40 mM KCl for 2 min at 20°C after synaptic and antibody labelling. For the TTX conditions, neurons were incubated with 1 µM TTX for either 10 min or 48 h at 37°C before synaptic and antibody labeling. For these recordings, the recording medium contained 1 µM TTX. For the long-lasting 48 h treatment, TTX was added at 8 DIV and neurons were tested at 10 DIV. All data (recording session) were taken within 20 min following primary antibody incubation to minimize endocytosis. For the TPA treatment, neurons were treated after synaptic and antibody labelings with either 100 nM TPA or with the inactive analogue, 100 nM

4- α -PHR (isophorbol) for 5 min at 20°C. The recording medium contained the same dose of TPA or 4- α -PHR used for the initial treatment. Calculation of the median diffusion was carried out on at least 2-4 different cultures, which correspond to approximately 25-50 different dendritic areas. Because antibody cross-linking may lower the diffusion of NMDARs, we compared the NMDAR diffusion distribution using different concentrations of anti-NR1 antibodies (data not shown). All diffusion distributions were similar suggesting that antibody cross-linking did not interfere with receptor diffusions.

Microscopy and single-molecule detection

A custom wide field single-molecule fluorescence inverted microscope equipped with a 100x oil-immersion objective (NA = 1.4) was used (IX70 Olympus, Bordeaux, France). The samples were illuminated for 30 msec at a wavelength of $\lambda = 532$ nm by a frequency doubled YAG laser (Coherent INC., Les Ulis, France) at a rate of 15 Hz. Use of a defocusing lens permitted illumination of a surface of $20 \times 20 \mu\text{m}^2$ with a mean illuminating intensity of 3 kW/cm^2 . An appropriate filter combination (DCLP550, HQ600/75, Chroma Technology, Brattleboro, USA) permitted the detection of individual fluorophore by a CCD camera system (Micromax, Princeton Instruments, Trenton, NY, USA). Using the same excitation path with another filter combination (DCLP650, HQ675/50, Chroma Technology, Brattleboro, USA), Red Deep Mitotracker (Molecular probes, Leiden, The Netherlands) was excited with the $\lambda = 633$ nm line of a He-Ne laser (JDS Uniphase, Manteca, CA, USA) at an illuminating intensity of $7 \pm 1 \text{ kW/cm}^2$. We imaged and resolved discrete fluorescence spots^{1,3-5}. Fluorescence spots exhibit one-step photobleaching and not gradual decay as for

ensemble photobleaching. The width of these spots corresponds to the point-spread function of the microscope and the signal originating from 350 ± 150 counts per 30 ms. Thus, only those fluorescence spots that have all the hallmarks of individual fluorescent molecules bound to GluR2 or NR1-containing receptors were retained for analysis¹. Only trajectories containing at least 4 points were retained. We calculated the instantaneous diffusion coefficient, D , for each trajectory, from linear fits of the first 4 points (first 3 points for trajectory of 4 frames) of the mean-square-displacement versus time function using $MSD(t) = \langle r^2 \rangle(t) = 4Dt$. The two-dimensional trajectories of single molecules in the plane of focus were constructed by correlation analysis between consecutive images using a Vogel algorithm⁶.

Determination of Endocytosis rate and impact on mobility measurements

Endocytosis rate was measured by immunohistochemistry¹. Briefly, live neurons were first incubated for 10 min with either the anti-GluR2 (BD Pharmingen) or anti-NR1 antibody at 37°C, washed, and then either fixed immediately with a 4% (w/v) paraformaldehyde solution (time zero) or incubated for 20 min at 37°C before fixation. To quantify surface versus endocytosed receptors, fixed neurons were first incubated for 45-60 min with 10 µg/ml with the secondary antibody, i.e. Alexa568 anti-mouse Ig or 10 µg/ml Alexa568 anti-rabbit IgG (Molecular Probes, Leiden, The Netherlands) to saturate cell surface bound primary anti-GluR2 and anti-NR1 antibodies respectively. Neurons were then permeabilized with 0.3% (v/v) Triton (X100) and incubated for 30 min with 5 µg/ml of the appropriate secondary antibodies as above to reveal endocytosed GluR2 and NR1 subunits respectively. Images were quantified using Metamorph Software (Universal Imaging, Downingtown, PA)⁷.

Control experiments¹ (data not shown) established that this procedure adequately specifically stains respectively surface and internalized receptors.

We found that $36 \pm 10\%$ of AMPARs ($n = 6$ neurons) and $17 \pm 4\%$ of NMDARs ($n = 6$ neurons) were endocytosed. This finding shows that the endocytosis rates of AMPAR and NMDAR are significantly different ($P < 0.05$, t -test). The extent of endocytosis is in agreement with other, earlier reports^{1,8,9}.

Mobility recordings were performed regularly from 0 to 20 min while the endocytosed pool was estimated at the end time, i.e. 20 min. Thus on average 18% of our recorded AMPARs (8.5% NMDARs) are endocytosed receptors. Unfortunately, we have no experimental way to determine for a given labeled receptor on live cells whether it is on the cell surface or internalized. However, we previously showed that endocytosed AMPARs pertain to the immobile pool of receptors¹. Since immobile AMPARs represent themselves 47% of the total receptors, the uncertainty induced by endocytosis is, in our control experimental conditions, in the order of 8%. This uncertainty is of 5% for NMDARs.

TPA treatment has been shown to increase GluR2-containing AMPAR endocytosis rate as well as to induce a redistribution of GluR2-containing AMPARs to synaptic sites¹⁰. In another set of experiments, we thus investigated the effect of TPA treatment on AMPAR endocytosis. In agreement with previous report¹⁰, TPA treatment (100 nM) significantly increased the amount of endocytosed AMPARs after 20 min incubation (control: $21 \pm 8\%$, $n = 6$ neurons; TPA: $55 \pm 11\%$, $n = 6$ neurons, $P < 0.05$, t -test). Thus, our measure of the AMPAR lateral mobility in this condition is likely biased by an increased proportion of internalized receptor, as we cannot distinguish between surface and internalised receptors. As above, the amount of bias

is approximately half these values. Thus, about 10.5% and 27.5% of recorded receptors are likely endocytosed in control and TPA mobility measurements, respectively. We expect a 17% increase in the percentage of immobile receptors due to endocytosed receptors¹. We found in mobility experiments that TPA increased the percentage of immobile receptors by 25% and decreased the mean diffusion coefficient of mobile receptors by 43% (from 0.39 in control conditions to 0.22 $\mu\text{m}^2/\text{s}$ in the presence of TPA, $n = 98$ and 61, respectively). Thus TPA both increases AMPAR endocytosis and decreases surface mobility.

In another condition, KCl treatment (40 mM, 2 min), that increased the AMPAR lateral diffusion, we found no significant change in the endocytosis rate (control: $21 \pm 8\%$, $n = 6$ neurons; KCl: $22 \pm 5\%$, $n = 6$ neurons, $P > 0.05$, t -test).

Supplementary Method References

1. Tardin, C., Cognet, L., Bats, C., Lounis, B. & Choquet, D. *Embo J.* **22**, 4656-4665 (2003).
2. Borgdorff, A.J. & Choquet, D. *Nature* **417**, 649-653 (2002).
3. Harms, G.S. et al. *Biophys. J.* **81**, 2639-2646 (2001).
4. Harms, G.S., Cognet, L., Lommerse, P.H., Blab, G.A. & Schmidt, T. *Biophys. J.* **80**, 2396-2408 (2001).
5. Schmidt, T., Schutz, G.J., Baumgartner, W., Gruber, H.J. & Schindler, H. *J. Phys. Chem.* **99**, 17662-17668 (1995).
6. Schutz, G.J., Schindler, H. & Schmidt, T. *Biophys. J.* **73**, 1073-1080 (1997).
7. Serge, A., Fourgeaud, L., Hemar, A. & Choquet, D. *J. Neurosci.* **22**, 3910-3920 (2002).
8. Lin, J.W. et al. *Nat. Neurosci.* **3**, 1282-1290 (2000).
9. Roche, K.W. et al. *Nat. Neurosci.* **4**, 794-802 (2001).
10. Chung, H.J., Xia, J., Scannevin, R.H., Zhang, X. & Huganir, R.L. *J. Neurosci.* **20**, 7258-7267 (2000).